Table 2 Comparison of C_L and C_D vs α between computations and experiments

		$\alpha = -1$ deg	$\alpha = -2$ deg	$\alpha = -3$ deg
C_L	Computations	0.268	0.120	−0.0151
	Experiments	0.259	0.130	0.0201
C_D	Computations	0.0259	0.0215	0.0205
	Experiments	0.0266	0.0213	0.0198

the root of sting. Perhaps separation is caused by the step between the fuselage edge and the sting, and this phenomenon strongly affects the calculation of drag. Both the lift and drag coefficients agree well with experimental data (see Table 2).

C. Cases for Series of Attack Angles

Table 2 shows the values of lift and drag coefficients for $\alpha = -1, -2$, and -3 deg. Except for the lift for $\alpha = -3$ deg, both the lift and drag coefficients agree well with experiments. It is especially remarkable that the computed drag corresponds well with wind-tunnel experiments, since, typically, in computations of aircraft flows the drag does not compare with the data.

IV. Concluding Remarks

The transonic flows about a fully configured model of aircraft named ONERA-M5 within the NAL transonic wind tunnel have been numerically solved to investigate the reliability of numerical solutions. The multidomain technique was used to solve the whole flowfield around the complicated configuration. In each domain the grid was generated by an algebraic method and the thin-layer Navier–Stokes equations were solved by the improved Chakravarthy–Osher TVD scheme. Further, a simple model was presented to estimate the outflow/inflow effects at the perforated wall of the transonic wind tunnel. The results obtained by the present methods have shown good coincidence with the experimental data of NAL wind-tunnel test, in regard to local C_p distributions on the main wing and total forces C_L and C_D.

Therefore, in spite of the primitive model for the perforated wind-tunnel wall and the immature algebraic turbulence model, we believe that this numerical analysis is the first step for the more precise evaluation of the numerical solutions and wind-tunnel experiments.

References

[1]Anon., "Experimental Data Base for Computer Program Assessment, Report of the Fluid Dynamics Panel Working Group 04," AGARD Rept. AR-138, 1979.

[2]Baldwin, B. S., Turner, J. B., and Knechtel, E. D., "Wall Interference in Wind Tunnels with Slotted and Porous Boundaries at Subsonic Speeds," NACA TN-3176, May 1954.

[3]Benek, J. A., Buning, P. G., and Steger, J. L., "A 3-D Grid Embedding Technique," AIAA Paper 85-1523, July 1985.

[4]Takakura, Y., and Ogawa, S., "Computations of Transonic Flows about a Fully Configured Model of Aircraft Using a Multi-Domain Technique," *Computers and Fluids* (to be published).

[5]Takakura, Y., and Ogawa, S., "A Simple Grid Generation Technique for Hypersonic Flow Around Complex Configuration," *Proceedings of the 9th NAL Symposium on Aircraft Computational Aerodynamics*, National Aerospace Lab. SP-16, Tokyo, Dec. 1991, pp. 9–14.

[6]Chakravarthy, S. R., and Osher, S., "A New Class of High Accuracy TVD Schemes for Hyperbolic Conservation Laws," AIAA Paper 85-0363, Jan. 1985.

[7]Takakura, Y., Ishiguro, T., and Ogawa, S., "On TVD Difference Schemes for the Three-Dimensional Euler Equations in General Coordinates," *International Journal for Numerical Methods in Fluids*, Vol. 9, No. 8, 1989, pp. 1011–1024.

[8]Wada, Y., Kubota, H., Ogawa, S., and Ishiguro, T., "A Diagonalizing Formulation of General Real Gas-Dynamic Matrices with a New Class of TVD Schemes," AIAA Paper 88-3596-CP, July 1988.

[9]Baldwin, B. S., and Lomax, H., "Thin Layer Approximation and Algebraic Model for Separated Turbulent Flows," AIAA Paper 78-257, Jan. 1978.

[10]Anon., "Fluid Motion," *Kagaku Kogaku Binran*, 5th ed., Kagaku Kogaku Kyokai, Tokyo, 1988, pp. 262–263.

Experimental Study of Perturbed Laminar Wall Jet

C. Shih* and S. Gogineni†
Florida A&M University and Florida State University, Tallahassee, Florida 32316

Introduction

A PLANE wall jet is a stream of fluid blown tangentially along a plane wall. It has a wide range of applications, such as boundary-layer control over a wing, film cooling on turbine blades, etc. It consists of two distinct regions: 1) an outer shear layer that is subjected to the inviscid Kelvin-Helmholtz instability and 2) an inner layer that behaves like a viscous boundary layer. The interaction between the structures from these two layers leads to the eventual laminar to turbulent transition. Katz et. al.[1] observed that the external excitation on the plane turbulent wall jet has no appreciable effect on either the maximum velocity decay or the spreading rate of the jet. The linear stability calculations by Cohen et. al.[2] indicated the existence of two unstable modes: an inviscid mode that represents the large-scale disturbances in the free shear layer, plus a viscous mode describing the small-scale disturbances near the wall. They have also shown that the relative importance of each mode can be controlled by subjecting the wall jet to small amounts of blowing or suction. The extensive literature available on wall jets is mainly based on either pointwise measurements, flow visualization studies, or analytical/numerical investigations. However, to understand the unsteady flow characteristics associated with the dynamic behavior of the vortices and their interactions, it is necessary to study the spatial vorticity distribution at each instant. In view of this, we proposed to examine the flowfield using particle image velocimetry (PIV). This technique can provide the instantaneous two-dimensional velocity data in a selected plane of the flowfield with sufficient spatial accuracy such that the instantaneous vorticity field can be obtained. For a detailed description of the PIV technique, please refer to Adrian[3] and Lourenco et al.[4]

The focus of the present investigation is to describe the effects of using a low-frequency, high-amplitude external acoustic excitation on a wall jet and the subsequent interactions between the inner and outer region vortical structures. Both PIV and smoke/laser sheet flow visualization techniques are used for the understanding of the global dynamics of the interaction process.

Experimental Setup

The experimental facility is shown schematically in Fig. 1. The wall jet originates from a two-dimensional channel ($h \times W \times L = 0.5 \times 10.0 \times 52.7$ cm) that is connected to a settling chamber via a two-stage contraction. The aspect ratio of the nozzle (W/h) is 20. Because of the long developing length of the channel ($L/h = 105.4$), the exit velocity profile is a fully developed parabolic profile. A loudspeaker attached to the settling chamber is used to perturb acoustically the wall jet (Fig. 1). The wall is made of Plexiglas plate with side walls to minimize the influence of the side edges. The jet is seeded with smoke particles produced by a Rosco-type 1500 smoke generator. The entire apparatus is placed inside an enclosure (1.5×1.5 m in cross section) with three sides covered by plastic sheets to minimize the outside influence. A second smoke generator of the same type is used to seed the outside ambient flow surrounding the jet. A Cartesian coordinate system (x, y, z) is chosen as shown in Fig. 1. A dual pulsed laser system consisting of two Spectra-Physics DCR-11 Nd:YAG pulsed lasers is used to provide the double illumi-

Received Aug. 22, 1994; revision received Oct. 10, 1994; accepted for publication Oct. 15, 1994.

*Associate Professor, Department of Mechanical Engineering, College of Engineering. Member AIAA.

†Research Assistant, Department of Mechanical Engineering, College of Engineering; currently NRC Postdoctoral Fellow, Aero Propulsion and Power Directorate, Wright Patterson AFB, OH 45433. Member AIAA.

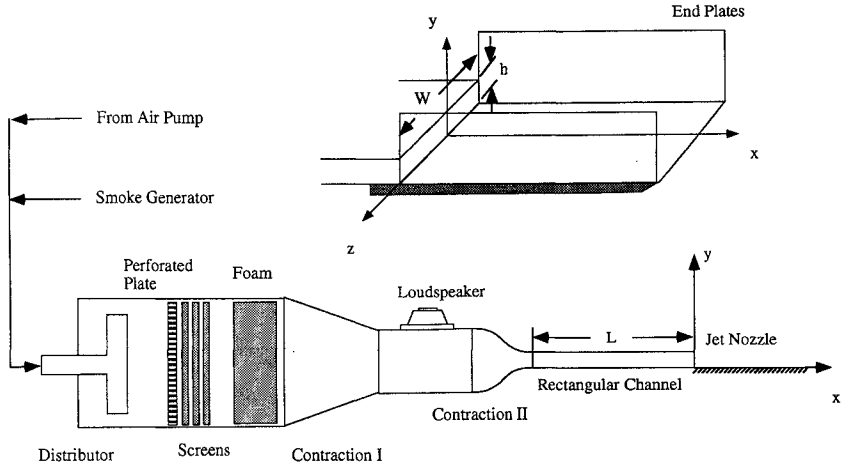

Fig. 1 Schematic of the wall jet facility.

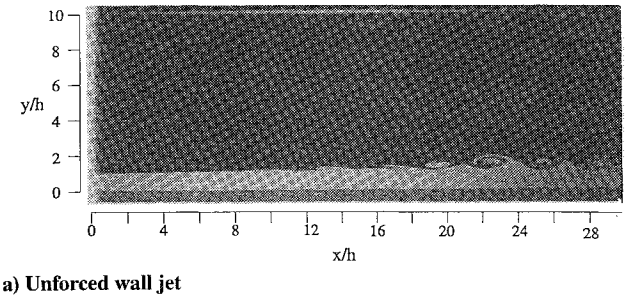

a) Unforced wall jet

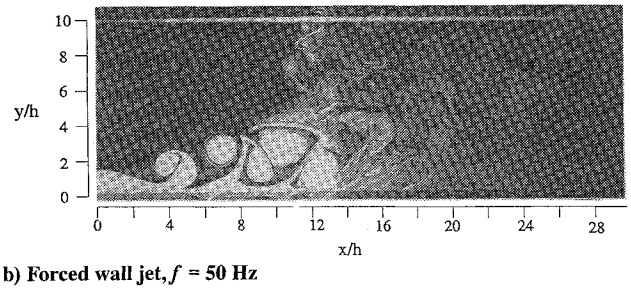

b) Forced wall jet, f = 50 Hz

Fig. 2 Flow visualization, comparison between unforced and forced wall jets.

nation pulses for PIV measurements. A phase-triggered electronic system is used to synchronize the temporal development of the wall jet flow to the external excitation.

Results and Discussion

It has been shown that as the shear layer vortices grow stronger under the influence of the external excitation, they can induce the detachment of the local boundary layer and accelerate the formation of the vortices in the inner region (Gogineni[5]). The strong interaction between the inner and outer region structures dominates the flow behavior and leads to the ejection of the boundary layer into the outer stream and to an early flow transition. This suggests that it is possible to manipulate the wall jet through external excitation. To effectively perturb the jet using the loudspeaker, a jet of low momentum with a mean velocity of 3 ± 0.1 m/s is used. The Reynolds number based on this mean velocity and the nozzle height h is 1000. For comparison purposes, the flow visualization picture corresponding to the unforced case is shown in Fig. 2a. The growth of instability waves and the subsequent emergence of discrete vortices in the outer shear layer can be clearly observed. The most amplified frequency of the instability wave, measured by a hot-wire anemometer and a spectrum analyzer, is 140 ± 1 Hz. The Strouhal number St_h, based on the most amplified frequency, jet height, and the mean exit velocity, is 0.233. However, these vortices are not strong enough to

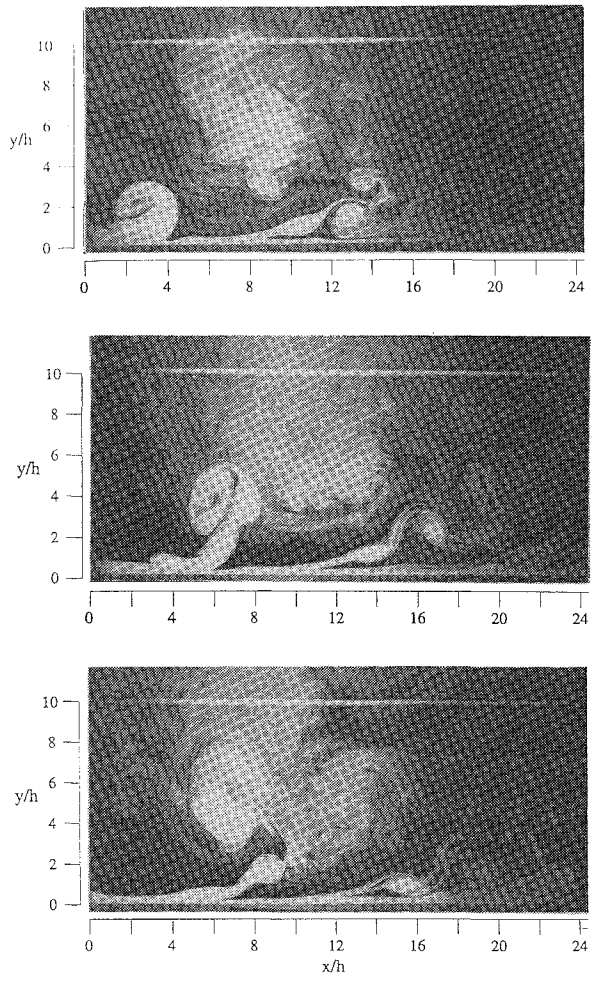

Fig. 3 Time development of a forced wall jet, f = 20 Hz.

interact with the boundary layer, and so the jet remains laminar if unforced.

When the jet is excited by a loudspeaker at a frequency of 50 Hz ($St_h = 0.083$) with high amplitude, the flow structure changes dramatically. Without excitation, the rms velocity fluctuation at the jet exit is 0.3% of the maximum exit velocity. The excitation produces a significantly higher fluctuation level in the center of the jet that is 10% of the maximum exit velocity. As a consequence, a massive vortex emerges in the shear layer under the influence of the acoustic perturbation. This vortex induces a detachment of the local boundary layer that leads to the formation and the ejection of a vortex from the inner layer. The inner region vortex interacts with the free

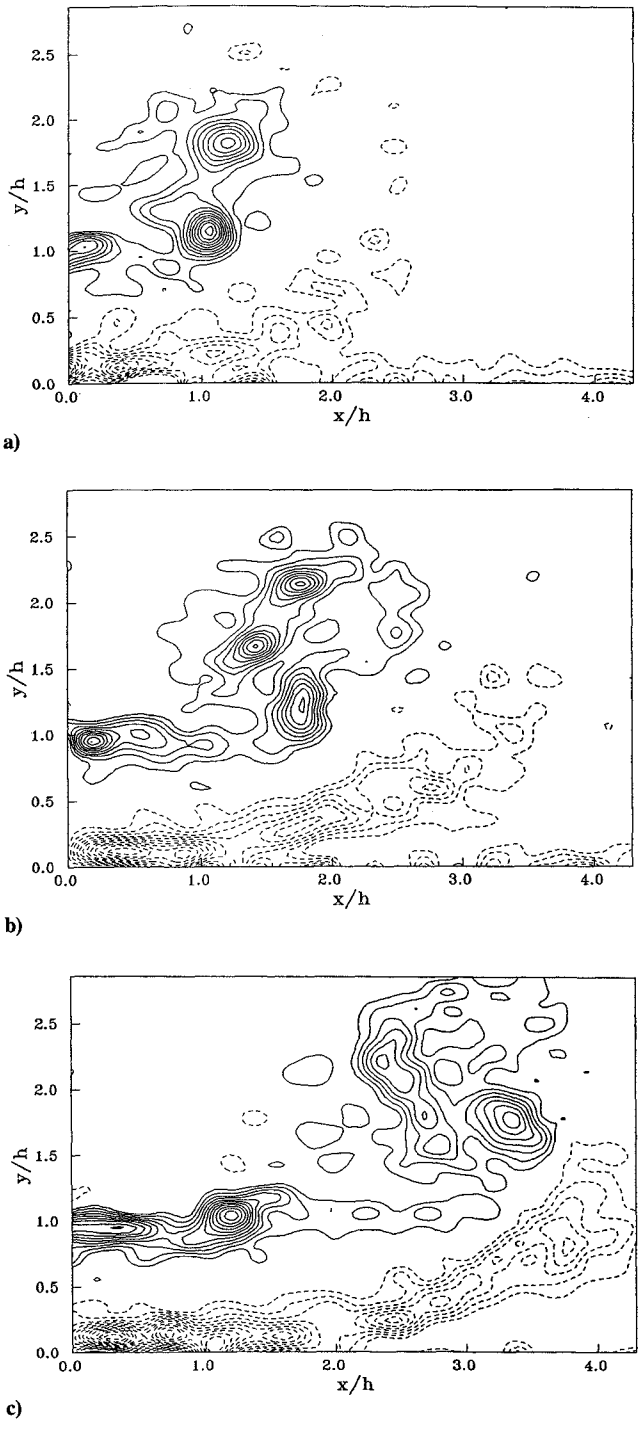

Fig. 4 Instantaneous PIV vorticity fields, 20-Hz forcing.

shear layer vortex and forms a mushroom-shaped counter-rotating vortex pair. Two such vortex pairs can be seen in Fig. 2b. Under the influence of the downstream vortex pair, a total breakaway of the upstream vortex pair from the surface is inhibited. However, as the downstream vortex pair begins to diffuse further downstream, there is a sudden ejection of the jet away from the wall followed by a rapid spreading of the jet and a transition to turbulence. The mechanism involved for the formation of the initial vortex in the inner region and the subsequent interactions between the inner and outer region vortical structures have been investigated by Gogineni.[5]

As shown by the previous observation,[5] the influence from the neighboring downstream vortex pair has a significant effect in preventing the complete ejection of the upstream vortex pair. This suggests that it is possible to enhance the flow control by varying the separation distance between vortex pairs. This can be achieved by forcing the jet at different frequencies. To reduce the mutual influence from the neighboring vortex pair, a lower frequency is required because it generates disturbance waves with a longer wavelength. Figures 3a–3c show a time sequence of the evolving wall jet when it is forced at a frequency of 20 Hz ($St_h = 0.033$). This forcing frequency is 1/7 of the natural instability frequency of an unforced jet at this Reynolds number. The initial vortex, which emerges as the shear layer responds to the external perturbation, appears to be more intense. It quickly induces the detachment of the inner layer from the wall and the formation of a counter-rotating vortex pair. This pair is propelled away from the wall and breaks down immediately. The trailing tail of the vortex pair rolls into a clockwise vortex and reattaches back on the wall after the head of the pair is ejected.

To quantify the response of the jet under forcing, PIV velocity measurements are made to examine the formation of the first vortex pair of the perturbed jet (20-Hz case). The associated vorticity fields are computed using a central finite difference scheme. A sequence of the PIV vorticity fields within one complete cycle is presented in Figs. 4a–4c. The solid contour lines represent counterclockwise vorticity, and the dashed lines represent clockwise vorticity. At the beginning of the sequence, the shear layer appears to be bent away from the wall. As shown in the vorticity field, multiple vortices coalesce into one large vortex. Underneath this vortex, the local boundary layer is lifting up and rolls into discrete vortices rotating in a clockwise sense (Fig. 4a). With the external excitation, the shear layer continues to develop at an amazingly fast rate that involves the coalescence of several discrete vortices into one large vortical structure (Figs. 4a–4c). A similar phenomenon has been observed by Ho and Huang[6] in their study of the development of the nonlinear shear layer instability of a plane mixing layer. They found that several shear layer vortices can coalesce into one large structure under very long wavelength and high-amplitude excitation. They referred to this phenomenon as the "collective interaction." In the present case, the emergence of one single massive vortex induces the immediate ejection of the boundary layer from the wall and formation of a clockwise vortex (Fig. 4b). The mutual induction between the counter-rotating vortices eventually propels the jet away from the wall (Fig. 4c). From PIV velocity field data (not shown here), the deflected jet inclines at an angle of 50 deg with respect to the wall at this instant. Further downstream, the jet can be deflected into a perpendicular standing position as shown in Fig. 3c.

Summary

The characteristic of a laminar wall jet under external excitation has been studied experimentally using PIV and flow visualization. In the outer shear layer, the vortical structure is greatly enhanced under external perturbation. The convecting shear layer vortical structure induces a sudden accumulation and ejection of wall vorticity into the outer flow. The strong interaction between the inner and outer structures in a form of counter-rotating vortex pair eventually leads to the complete ejection of the wall jet flow and an immediate transition to turbulence. In light of this interaction, low-frequency perturbation is used to effectively deflect the wall jet and promote its growth and transition.

References

[1]Katz, Y., Horev, E., and Wygnanski, I. J., "The Forced Turbulent Wall Jet," *Journal of Fluid Mechanics*, Vol. 242, 1992, pp. 577–609.

[2]Cohen, J., Amitay, M., and Bayly, B. J., "Laminar-Turbulent Transition of Wall Jet Flows Subjected to Blowing and Suction," *Physics of Fluids A*, Vol. 4, No. 2, 1992, pp. 283–289.

[3]Adrian, R. J., "Particle Imaging Techniques for Experimental Fluid Mechanics," *Annual Review of Fluid Mechanics*, Vol. 23, 1991, pp. 261–304.

[4]Lourenco, L., Krothapalli, A., and Smith, C. R., "Particle Image Velocimetry," *Lecture Notes in Engineering: Advances in Fluid Mechanics Measurements*, edited by M. Gad-el-Hak, Springer-Verlag, New York, 1989, pp. 128–199.

[5]Gogineni, S., "Particle Image Velocimetry Study of Two Dimensional Transitional Plane Wall Jet," Ph.D. Thesis, Florida State Univ., Tallahassee, FL, Dec. 1993.

[6]Ho, C. M., and Huang, L. S., "Subharmonics and Vortex Merging in Mixing Layers," *Journal of Fluid Mechanics*, Vol. 119, 1982, pp. 443–473.